Calculation of electrical resistivity produced by dislocations and grain boundaries in metals

1994 J. Phys.: Condens. Matter 6 873

(http://iopscience.iop.org/0953-8984/6/4/007)

J. Phys.: Condens. Matter 6 (1994) 873–886. Printed in the UK

Calculation of electrical resistivity produced by dislocations and grain boundaries in metals

A S Karolik and A A Luhvich

Institute of Applied Physics, Academy of Sciences of Byelarus, 16 F Skaryna Street, Minsk 220072, Republic of Byelarus

Received 6 May 1993, in final form 25 August 1993

Abstract. The partial-wave method is used for the calculation of the residual electrical resistivity caused by dislocations and grain boundaries in various metals. The dislocation core is regarded as a resonance scattering line defect containing surplus free volume. Scattering by elastic distortions of the lattice is neglected. An estimation of the effective carrier concentration in transition metals is performed on the basis of Mott's theory. The proposed model for the evolution of the grain-boundary structure with misorientation angle regards the approach and confluence of the line defects forming the boundary, and results in a decrease of the resonance part of the total scattering cross section. The high-angle grain boundaries are assumed to consist of cylindrical voids. Taking into account the values of the steady Burgers' vectors, quite satisfactory agreement with the available experimental data is obtained.

1. Introduction

Dislocations and grain boundaries are the most widespread defects in metals, playing a leading role in the processes of plastic deformation. The explanation of the high residual electrical resistivity of dislocations and grain boundaries, begun a few decades ago, has met with certain difficulties until now. The first calculations of the residual resistivity connected with dislocations (ρ_d) and grain boundaries (ρ_g) in simple metals yielded values 1–2 orders of magnitude lower than the experimental ones [1–4]. It has been shown that scattering of conduction electrons by long-range elastic strain fields surrounding the dislocation is negligible and contributes a few per cent to the general value of the dislocation resistivity [2, 5]. Taking into account the lattice dilatation during plastic deformation and the fact that the distortion is concentrated mainly in the dislocation core resulted in the right order of magnitude of the residual resistivity produced by dislocations [6]. However, in the framework of this model, it was impossible to explain the other experimental facts connected with dislocations in metals, such as the contribution of dislocations to the thermoelectric power and also the temperature dependence of the dislocation residual resistivity.

Further progress in investigation of the influence of dislocations on electron-transfer properties was associated with the consideration of virtual quasi-stationary states [7–9, 13], the existence of which had been predicted theoretically [10] and later observed experimentally [11]. The resonance scattering of conduction electrons by quasi-stationary states lying close to the Fermi surface gave ρ_d values close to the experimental ones for a great number of metals [7]. The best accord was obtained for non-transition metals. Representing the grain boundary by a set of resonance scattering dislocations, the contribution of the grain boundaries to the residual resistivity was calculated in satisfactory agreement with the experiment in order of magnitude for non-transition metals [12].

0953-8984/94/040873+14$07.50

However, some works [7, 10, 12] were criticized both for the uncertainty in the nature of the disturbance causing the resonance and for the independence of the results on the type of dislocations and the value of their Burgers' vector. It must be pointed out that the dislocation description of grain boundaries is correct only for low-angle boundaries with misorientation angle $\theta < 15°$. In the high-angle range, the dislocation cores convert into cylindrical pores [15], whereas in [12] the dislocation description has been used over all the range of misorientation. The calculations have been performed for the particular case of columnar structured thin films, when the dislocations constituting the boundary are all perpendicular to the current flow and thus make a maximum contribution to the residual resistivity.

In one of the latest works [14] it was suggested that the high electrical resistivity of dislocations is due to the Bragg reflection of Fermi electrons from the Brillouin zone faces resulting in large-angle scattering. Using a fitting parameter, quite satisfactory agreement with experiment for 16 metals has been obtained. However, the existence of such deformations near the dislocation core at which all Fermi surfaces would touch the Brillouin zone faces seems doubtful, especially so for monovalent metals.

Earlier we carried out a calculation of the residual resistivity and additional thermoelectric power due to dislocations and grain boundaries in the noble metals with allowance for the expansion of the lattice close to the dislocation core as well as the existence of quasi-stationary resonance states near to the Fermi energy [9, 16]. Satisfactory agreement with the experimental data has been obtained. In this work a more improved model of the dislocation core and of the grain-boundary structure is proposed and a broader range of metals is considered. Besides noble metals, other monovalent and also more complicated polyvalent and transition metals having FCC, BCC and HCP structure are considered.

The paper is organized in the following way. It consists of two main parts. In the first (section 2) we consider the model, present the basic expressions and give the results for dislocations in metals. Here the effective carrier concentration is introduced. In the second part (section 3) we discuss the grain-boundary model, its change with the angle of misorientation, and give the results of the calculation of the residual resistivity due to grain boundaries for a range of misorientation angles. In section 4 a discussion of the results and comparison with experiment is given.

2. The dislocation residual resistivity

In this paper, calculation of the scattering cross section for line defects is performed in the free-electron approximation using the partial-wave method. We take into account only scattering by the line defect cores. Scattering of electrons by the elastic strain fields is neglected because of their minor influence on the resistivity. The lattice dilatation connected with both edge and screw dislocations is concentrated mainly in the area of the core. According to the estimates of different authors, the value of the dilatation dV lies in the interval from b_B^2 to $4b_B^2$ per unit length of dislocation (where b_B is the Burgers' vector) [17, 18]. This free volume creates a negative surplus charge in comparison with the ideal lattice. Side by side with the expanded area there is a compressed region bearing local positive charge, which can seize the conduction electrons for a short time and form quasi-stationary states. Such states lying close to the Fermi energy have been used in [11] for a description of the measured dependence of the dislocation residual resistivity on temperature and on the stage of deformation.

In the partial-wave method the task of electron scattering reduced to the solution of the Schrödinger equation for the axial–cylindrical potential

$$V(r) = \begin{cases} -V & r < r_1 \\ V_0 & r_1 \leqslant r \leqslant r_2 \\ 0 & r > r_2. \end{cases} \tag{1}$$

Such a form of potential is the simplest that permits one to take into account the main features of the perturbation of the crystal lattice in the region of the dislocation core, i.e. the repulsion of the electrons by the negative charge and the existence of resonance states in the area of positive values of energies. The same form of potential has been obtained in [19] for a screw dislocation in potassium within the framework of the pseudopotential concept, taking account of the displacement of atoms in the area of the core and the deformation of the elastic continuum of the surrounding matrix. The external radius of the potential r_2 was taken as equal to the atomic one, and the internal radius r_1 conditionally was put at $r_1 = r_2/2$, which did not considerably affect the results.

In view of the fact that the dislocation length L is much greater than its width $2r_2$, edge effects do not need to be taken into account, and the dislocation may be regarded as an infinitely long defect. This is the reason why only the perpendicular component of the wavevector $k_\perp = k \sin\phi$ is changed during the scattering (here k is the wavevector at the Fermi level and ϕ is the angle between the dislocation axis and the vector k).

After separation of variables, the radial part of the Schrödinger equation is reduced to the Bessel equation

$$R''r^2 + R'r + \left[\left(k_\perp^2 - \frac{2m}{\hbar^2}V(r)\right)r^2 - n^2\right]R = 0 \tag{2}$$

the solution of which are Bessel functions with arguments κr, $\kappa_0 r$ and $k_\perp r$ in the regions $r < r_1$, $r_1 \leqslant r \leqslant r_2$ and $r > r_2$ respectively, where

$$\kappa = (k_\perp^2 + 2mV/\hbar^2)^{1/2}$$

and

$$\kappa_0 = (k_\perp^2 - 2mV_0/\hbar^2)^{1/2}.$$

The general solution may be written in the form

$$\psi(r, \theta, \phi) = \sum_{n=0}^{\infty} \frac{C_n}{(k_\perp r)^{1/2}} \cos(k_\perp r - \tfrac{1}{2}n\pi - \tfrac{1}{4}\pi + \eta_n)e^{in\phi} \tag{3}$$

where η_n is the phase shift of the asymptotic solution of the nth radial function in the perturbed state relative to the unperturbed one. A detailed description of the resonance scattering of electrons by a line defect with a potential of form (1) at $V = 0$ has been presented [9]. Here we give only the main results necessary for subsequent analysis and formulae differing from the coresponding ones in [9].

The phase shift η_n can be represented as a sum of potential α_n and resonance β_n components:

$$\eta_n = \alpha_n + \beta_n \tag{4}$$

where

$$\beta_n = \tan^{-1}\left(\frac{\Gamma_n}{2(E_{rn} - k_\perp^2)}\right)$$

and E_{rn} and Γ_n are the position and width of the nth resonance level. Demanding continuity of the wavefunction and its derivative at $r = r_1$ and $r = r_2$ we get the expression for the potential phase

$$\alpha_n = \tan^{-1}(A_n/B_n) \tag{5}$$

where

$$\begin{aligned} A_n = {} & \kappa k_\perp \{J_n'(\kappa r_1) J_n'(k_\perp r_2)[I_n(\kappa_0 r_2) K_n(\kappa_0 r_1) - I_n(\kappa_0 r_1) K_n(\kappa_0 r_2)]\} \\ & + \kappa \kappa_0 \{J_n'(\kappa r_1) J_n(k_\perp r_2)[I_n(\kappa_0 r_1) K_n'(\kappa_0 r_2) - I_n'(\kappa_0 r_2) K_n(\kappa_0 r_1)]\} \\ & + \kappa_0 k_\perp \{J_n(\kappa r_1) J_n'(k_\perp r_2)[I_n'(\kappa_0 r_1) K_n(\kappa_0 r_2) - I_n(\kappa_0 r_2) K_n'(\kappa_0 r_1)]\} \\ & + \kappa_0^2 \{J_n(\kappa r_1) J_n(k_\perp r_2)[I_n'(\kappa_0 r_2) K_n'(\kappa_0 r_1) - I_n'(\kappa_0 r_1) K_n'(\kappa_0 r_2)]\} \end{aligned}$$

and B_n is obtained by substitution of the functions $J_n(k_\perp r_2)$ and $J_n'(k_\perp r_2)$ by $N_n(k_\perp r_2)$ and $N_n'(k_\perp r_2)$ respectively.

The determination of the resonance phase β_n is reduced to finding the energy eigenvalues under the condition of the existence of only a divergent electron wave at the asymptote, which corresponds to disintegration of the state. To this end we deal with the complex energy $\tilde{E}_\perp = E_r - i\Gamma/2$ and with the complex wavevectors

$$\tilde{k} = 2m\tilde{E}_\perp/\hbar^2$$

$$\tilde{\kappa} = (\tilde{k}^2 + 2mV/\hbar^2)^{1/2}$$

$$\tilde{\kappa}_0 = (\tilde{k}^2 - 2mV_0/\hbar^2)^{1/2}.$$

The precise solutions of equation (2) finite at the origin are given by

$$\begin{aligned} R_1 &= J_n(\tilde{\kappa} r) \qquad r < r_1 \\ R_2 &= B_1^n I_n(\tilde{\kappa}_0 r) + B_2^n K_n(\tilde{\kappa}_0 r) \qquad r_1 \leqslant r \leqslant r_2 \\ R_3 &= C_1^n H_n^1(\tilde{k}_\perp r) \qquad r > r_2. \end{aligned} \tag{6}$$

The condition of continuity of the solutions yields the equation

$$\begin{aligned} & [\tilde{\kappa}_0 I_{n+1}(\tilde{\kappa}_0 r_2) H_n^1(\tilde{k} r_2) + \tilde{k} I_n(\tilde{\kappa}_0 r_2) H_{n+1}^1(\tilde{k} r_2)][\tilde{\kappa}_0 K_{n+1}(\tilde{\kappa}_0 r_1) J_n(\tilde{\kappa} r_1) - \tilde{\kappa} K_n(\tilde{\kappa}_0 r_1) J_{n+1}(\tilde{\kappa} r_1)] \\ & \quad = [\tilde{\kappa}_0 K_{n+1}(\tilde{\kappa}_0 r_2) H_n^1(\tilde{k} r_2) - \tilde{k} K_n(\tilde{\kappa}_0 r_2) H_{n+1}^1(\tilde{k} r_2)][\tilde{\kappa}_0 I_{n+1}(\tilde{\kappa}_0 r_1) J_n(\tilde{\kappa} r_1) \\ & \qquad + \tilde{\kappa} I_n(\tilde{\kappa}_0 r_1) J_{n+1}(\tilde{\kappa} r_1)]. \end{aligned} \tag{7}$$

Its roots give the energies and widths of the resonance levels E_{rn} and Γ_n and therefore the resonance phase shifts β_n. The localization of the resonance states depends on the depth of the potential well V. We believe that the conduction electrons will interact with the resonance levels most intensively when the levels are located close to the Fermi energy within the thermal scatter $k_B T$. That is why the parameter V was fitted in such a manner to provide the condition

$$|E_{rn} - E_F| \leqslant k_B T. \tag{8}$$

The calculations show that, if the zero level satisfies the condition, the others are so far removed that they may be left out of account. So we believe $\beta_n = 0$ at $n > 1$. In the following we drop the zero index n on E_{rn} and Γ_n.

The transport cross section for the normal component of the wavevector $k_\perp$ can be expressed as a sum of three constituents (resonance R, potential P and interference I), each of which exhibits a different character of interaction of the electron wave with the defect:

$$\begin{aligned} Q_\perp &= \frac{4}{k_\perp}\sum_{n=0}^{\infty}\sin^2(\eta_n - \eta_{n+1}) \\ &= \frac{1}{k_\perp}\left(\frac{\Gamma^2}{(E_\perp - E_r)^2 + \Gamma^2/4} - \frac{2[\Gamma^2 \sin\delta_0 - \Gamma(E_\perp - E_r)\sin(2\delta_0)]}{(E_\perp - E_r)^2 + \Gamma^2/4}\right. \\ &\quad \left. + 4\sum_{n=0}^{\infty}\sin^2\delta_n\right) \\ &\equiv R_\perp + I_\perp + P_\perp \end{aligned} \tag{9}$$

where $E_\perp = \hbar^2 k_\perp^2/2m$ and $\delta_n = \alpha_n - \alpha_{n+1}$.

The total transport cross section averaged over all the possible directions of the wavevector relative to the dislocation axis is given by

$$Q = \tfrac{1}{2}\int_0^\pi (\sin\phi) Q_\perp(\phi)\,\mathrm{d}\phi = \frac{2}{k_\perp}\int_0^\pi \sum_{n=0}^{\infty}\sin^2(\eta_n - \eta_{n+1})\,\mathrm{d}\phi. \tag{10}$$

The residual resistivity due to a dislocation per unit of its density is calculated in the relaxation-time approximation using the expression

$$\rho_d/N_d = \hbar k Q/n_e e^2 \tag{11}$$

where n_e is the carrier concentration.

The height of the potential barrier V_0 is determined from the Friedel sum rule to provide self-consistency of the potential with the screened charge. For line defects the rule can be written in the form [2]

$$\xi = \frac{2k}{\pi^2}\int_0^\pi \eta_n \sin\phi\,\mathrm{d}\phi \tag{12}$$

where ξ is the line density of surplus charge along the dislocation axis, expressed by a quantity of electron charge. The condition (12) was fulfilled with an accuracy of 10^{-2}; the

number n is limited by $n = 6$. The value of dilatation into the dislocation core is taken as $dV = b_B^2$ [18], from which the value ξ is determined as $\xi = n_s\,dV/\Omega$, where n_s is the number of carriers per atom and Ω is the atomic volume. As the value b_B we take the steady Burgers' vector of the full dislocation for the corresponding crystal structure. Thus, in FCC metals the value b_B is equal to $\frac{1}{2}\langle 110\rangle$ or $a\sqrt{2}/2$; in BCC metals, $\frac{1}{2}\langle 111\rangle$ or $a\sqrt{3}/2$; in HCP, $\frac{1}{3}\langle 11\bar{2}0\rangle$ or a (where a is the lattice parameter).

The value of the wavevector at the Fermi level is calculated on the basis of the free-electron approximation $k = (3\pi^2 n_s/\Omega)^{1/3}$. As the carrier concentration n_e in (11), the concentration of those carriers is taken which effectively take part in the processes of scattering by defects, i.e. those which are not excluded from the processes by other competing scattering mechanisms proceeding with much higher probability. So

$$n_e = n_s^*/\Omega$$

where n_s^* is the effective number of carriers per atom.

Now we shall dwell upon the estimation of the value n_s^* in detail. For monovalent and polyvalent non-transition metals we assume $n_s^* = n_s$. For transition metals the evaluation of the number n_s is made on the basis of Mott's theory, taking into account the features of the electron energy structure of the metals. In these metals there are two partially filled overlapping bands (s and d) near the Fermi energy. By reason of the narrowness of the d zone and its high occupation, the d holes do not take part in the transfer processes, but they are effective scatterers of s electrons because of the high probability of s–d transitions. The theory suggests that the number of electrons with spin up ($\uparrow$) in the s zone is equal to the number of electrons with spin down ($\downarrow$), and the scattering of s electrons into free s and d states occurs without spin overturn. Such an assumption is valid in the lowest order of perturbation theory under the condition of neglecting spin–orbit interaction.

Thus in metals that have one d subband ($\uparrow$) filled completely and the other one ($\downarrow$) partially empty, it is natural to assume [21] that the effective number of current carriers in the s zone is $n_s^* = n_s/2$. Thus s electrons with spin down are scattering on the vacant states of the d $\downarrow$ subband and only s electrons with spin up are taking part in the process of scattering on defects. Such an approach has been used in [21] for estimating the effective concentration of carriers in metals at the end of the transition series (Ni, Co), in the case when the density of states at the Fermi level in the d zone is much greater than the respective parameters in the s zone, that is $N_d \gg N_s$. In this case the carrier concentration was determined from the average atomic magnetic moment per atom μ. So for nickel, which has $\mu = 0.54\mu_B$ at 10 (s+d) electrons per atom, the carrier concentration in the s zone was $n_s = 0.54$ e/atom and as many holes in the d zone. In cobalt, with nine (s+d) electrons, $\mu = 1.72\mu_B$ and $n_s = 0.72$ e/atom.

However, for metals at the beginning and in the middle of the transition series (in the present paper thay are Ti, Zr, Mo and W) having vacant states in both subzones, it would be more correct to admit that the scattering probability of s electrons into vacant states of s and d zones is proportional to the density of states in these zones at the Fermi energy. Thus taking into account that in the τ approximation

$$1/\tau_s = 1/\tau_{sd} + 1/\tau_{ss}$$

where τ is the relaxation time of the respective process of scattering, and assuming that the coupling constants are the same, it appears that the relaxation velocities τ_{ss}^{-1} and τ_{sd}^{-1} are proportional to the density of states at the Fermi level, N_s and N_d respectively. So

the total number of s electrons n_s with spin up and down will be divided into two parts $n_s = n_{sd} + n_{ss}$ in proportion $n_{sd}/n_{ss} = N_d/N_s$, from which only n_{ss} will participate in the processes of scattering on lattice defects. That is, the effective number of carriers is $n_s^* = n_{ss}$. The values n_s and n_s^* used here are given in table 1 for the metals considered with an indication of the lattice constants, the crystal structures and the group numbers in the periodic system. The quantities n_s for metals Be, Zn, Cd, Al, Ti, Zr, Mo, W and Pd are taken from the zone-structure calculation, the results of which are generalized in [7]. The atomic magnetic moment of Fe was taken equal to $\mu = 2.22\mu_B$. In accordance with Hund's rule one d subband (↑) is assumed to be filled completely, so that the magnetic moment of Fe determined the number of d holes in the other d subband (↓). The effective number of carriers n_s^* for Ti, Zr, Mo and W was estimated by using experimental data on electron specific heat, which were proportional to the density of electron states on the Fermi level as a first approximation. In conformity with the data listed in [22], the specific heat γ for Ti, Zr, Mo and M respectively is equal to 8.1×10^{-4}, 6.9×10^{-4}, 5.0×10^{-4} and 2.68×10^{-4} cal mol^{-1} K^{-2} (this is the arithmetic mean value from the experimental row cited in [22]). If these quantities are divided by the value $\gamma_{Cu} = 1.66 \times 10^{-4}$ cal mol^{-1} K^{-2}, we obtain the corresponding density of electron states at the Fermi energy N_{s+d} in units of the density of states of copper. It is possible to estimate the density of states in the s zone for these metals relative to copper on the basis of the free-electron model assuming $N_s \sim n_s^{1/3}$. In such a way the density of states in the s zone (N_s) constitutes correspondingly for Ti, Zr, Mo and W values 0.40, 0.40, 0.76 and 0.62. Hence one can evaluate the quantities $n_{ss} = n_s^*$ by the expression $n_{ss} = N_s n_s / N_{d+s}$; these values are presented in table 1.

Table 1. Parameters of crystalline structure and number of carriers per atom.

			Lattice constants			
Metal	Group	Structure	a (Å)	c (Å)	n_s	n_s^*
Na	IA	BCC	4.23		1	1
K	IA	BCC	5.23		1	1
Cu	IB	FCC	3.62		1	1
Ag	IB	FCC	4.09		1	1
Au	IB	FCC	4.08		1	1
Be	IIA	HCP	2.29	3.58	0.032	0.032
Zn	IIB	HCP	2.66	4.95	0.09	0.09
Cd	IIB	HCP	2.98	5.62	0.095	0.095
Al	IIIB	FCC	4.05		1	1
Ti	IVA	HCP	2.95	4.69	0.065	0.0054
Zr	IVA	HCP	3.23	5.15	0.065	0.0064
Mo	VIA	BCC	3.15		0.44	0.112
W	VIA	BCC	3.16		0.24	0.097
Fe	VIII	BCC	2.87		0.22	0.11
Co	VIII	HCP	2.51	4.07	0.72	0.36
Ni	VIII	FCC	3.52		0.54	0.27
Pd	VIII	FCC	3.89		0.55	0.275
Pt	VIII	FCC	3.92		0.42	0.21

The results of calculations of the residual resistivity due to dislocations per unit density (ρ_d/N_d) are listed in table 2. The calculated parameters of the potential (1), V and V_0, are represented there as well. For comparison we represent here the results of previous works and also the available experimental data.

Table 2. Calculated parameters of the scattering potential and dislocation specific resistivity.

			ρ_d/N_d (10^{-19} Ω cm^3)			
				Previous works		
Metal	V_0	V	This work	[20]	[14]	Experimental data
Na	8.1	3.0	6.9			
K	7.1	3.6	11.3	8.1 2.5–8.1 [19]	5.1	4 [31]
Cu	21.4	10.3	1.9	1.3	0.78	1.6 ± 0.2 [7] 1.8–2.3 [35,30] 1.7 [36]
Ag	16.9	8.1	2.7	1.9	1.1	1.9 [31] 3.1 [37]
Au	16.6	8.0	2.6	1.9	1.2	2.6 [31]
Be	50.7	27.1	21.7	28	22	34 [7]
Zn	30.0	18.3	15.8			
Cd	23.8	14.5	21.5	25	7.3	24 [7]
Al	17.2	8.3	2.7	1.8	1.0	1.8 ± 0.1 [38] 3.2 [31]
Ti	25.7	15.0	301.4	29		100 [7]
Zr	21.4	12.7	330.2	40	15	~ 100 [31]
Mo	20.0	12.9	17.3	3.7	3.8	5.8 [7] 22 [32]
W	22.4	14.8	17.8	7.4	6.1	7.5 [7] 19 [31,33]
Fe	19.1	12.5	12.6	1.9	1.9	10 ± 4 [7]
Co	22.9	12.9	4.5			
Ni	23.3	14.3	5.4	1.1	3	9.4 [31] 2.8 ± 0.5 [14]
Pd	19.1	11.6	7.2			
Pt	19.5	12.4	9.0	4	2.5	~ 9 [31]

3. The grain-boundary residual resistivity

The structure of low-angle grain boundaries, that is, boundaries with an angle of misorientation $\theta < 15°$, is sufficiently well understood now. To represent a simple symmetrical tilt boundary in a cubic lattice, one set of edge dislocations is sufficient, with Burgers' vector b_B a distance D apart

$$D = b_B/[2\sin(\theta/2)]. \tag{13}$$

In the general case, an asymmetrical low-angle boundary having both tilt and twist components can be made up by three independent sets of dislocations with non-coplanar Burgers' vectors. In this paper, for the purpose of simplicity, we shall deal with symmetrical tilt grain boundaries around the directions ⟨100⟩ for FCC, ⟨110⟩ for BCC and ⟨0001⟩ for HCP structures. In HCP crystals the distance between line defects can be expressed as

$$D = b_B \sin(\pi/3 - \theta/2)/[2\sin(\theta/2)] \tag{14}$$

taking into account that a slip happens most often along the most packed planes {0001}. The value b_B is assumed to be equal to $a\sqrt{2}/2$, $a\sqrt{3}/2$ and a for FCC, BCC and HCP structures respectively. The dislocation density into grain boundaries increases with the misorientation angle, and at $\theta > 20°$ the dislocation concept cannot be used. There are quite a number of high-angle grain-boundary models, and reviews can be found in [23] and [24]. They are the partial dislocation model, the bubble raft model, the dislocation core model, the disclination model, the island model, the structural unit model and others. The general feature of these theories is the representation of the fact that the high-angle boundary is more porous and friable in comparison with the low-angle one. However, it remains unclear what will happen after the dislocations draw together to a distance of a few atoms apart, when they begin to interact with each other. The model of the transformation of grain-boundary structure with misorientation angle proposed here allows one to realize a gradual transfer from resonance scattering dislocations to potential scattering cylindrical voids. It may be regarded as a further development of the dislocation core model first put forward in [25].

The model proposed here is shown schematically in figure 1. In the low-angle range (area I) the grain boundary is presented by dislocations with steady Burgers' vector b_B. As the misorientation angle increases, the separation between the dislocations decreases. When the separation becomes less than a critical value D_c, the dislocations start agglomerating into superdislocations with Burgers' vector b (area II). The critical distance D_c may be connected with the critical angle θ_c using (13) or (14). In accordance with [26] the confluence of head dislocations squeezed by external stress becomes energy advantageous if the distance between them is equal to $D < (7\text{–}10)b_B$. In this work the critical distance is $D_c = 7b_B$, the corresponding critical angle θ_c in cubic and hexagonal structures is 8° and 7° respectively. The process of dislocation confluence will be irregular in real crystals; nevertheless, one can speak about enhancement of average Burgers' vector of superdislocations b from the beginning of the process. In cubic crystals let the value b change with θ by the law

$$b = 2D_c \sin(\theta/2) \tag{15}$$

and in HCP crystals

$$b = 2D_c[2\sin(\theta/2)/\sin(\pi/3 - \theta/2)]. \tag{15a}$$

As shown in [27] this process is accompanied by a decrease in the amount of resonance scattering in the total cross section. At an angle θ^* the resonance part of the cross section

$$Q_R = \tfrac{1}{2}\int_0^{\pi} (\sin\phi) R_\perp(\phi)\, d\phi$$

will be far less than the total value Q and it may be neglected. From this moment, the grain boundary is regarded as a high-angle one in our model (the area III in figure 1). Let the angle

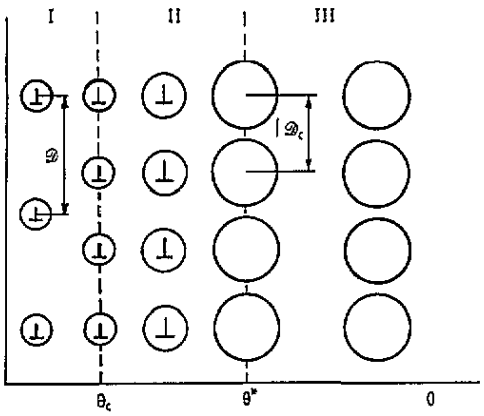

Figure 1. The scheme of changing of the grain-boundary structure with the misorientation angle: I, low-angle area; II, transition area; III, high-angle area. D_c and θ_c, the critical distance and the corresponding critical angle starting from the dislocations agglomerate into superdislocations. θ_c, limiting angle at which the fraction $Q_R/Q \leqslant 0.01$.

θ^* be called a limiting one. The value θ^* is the angle at which the fraction $Q_R/Q < 0.01$. Thus, within the large-angle area the grain boundary turned out to consist of cylindrical voids. A similar picture follows from [28], in which it was shown that enhancement of misorientation is accompanied by an intense growth of the grain-boundary core width until high angle, where the concept of dislocation fails.

We believe that the structure of the high-angle boundary and the parameters of the line defect cores inside it do not change practically with the misorientation angle. It is confirmed by the angle independence (or insignificant dependence) of the interfacial energy in the high-angle area if there are no special misorientations. Special grain boundaries with high density of coincident sites are characterized by sharp cusps in the energy–angle dependence. Observation of the misfit dislocations in special boundaries indicates that their structure is close to that of the low-angle ones. Thus, the model proposed here can be used for consideration of grain-boundary evolution between two adjacent special misorientations.

In this work we neglect the interaction of line defects in the boundary. This is justified by the fact that the electrostatic interaction, because of screening effects, does not influence very much the potentials of neighbouring defects more than a few atomic distances away, and the interaction through the long-range strain fields contributes to the resistivity about two orders of magnitude less compared with that of the dislocation core [29].

Thus, knowing the resistivity of line defects constituting the boundary ρ_L/N_L (dislocations, superdislocations or cylindrical voids) and the distances between them D, one can calculate the grain-boundary resistivity per unit area in unit volume of a polycrystalline material

$$\rho_g/N_g = \rho_L/N_L D \tag{16}$$

where N_L is the line defect density. For cubic structures

$$\rho_g/N_g = 2\rho_L \sin(\theta/2)/N_L b \tag{17}$$

where

$$b = \begin{cases} b_B & \theta < \theta_c \\ D_c \sin(\theta/2) & \theta_c \leqslant \theta \leqslant \theta^* \\ D_c \sin(\theta^*/2) & \theta^* \leqslant \theta \leqslant \theta_s/2. \end{cases}$$

For hexagonal close-packed crystals analogous expressions are derived from (14) and (15*a*). The angle θ_s is connected with the periodicity of the structure. So $\theta_s = \pi/2$ for cubic structures and $\theta_s = \pi/3$ for HCP ones. The maximal misorientation angle is thus $\theta_s/2$.

The residual resistivity per unit density of line defects ρ_L/N_L is defined by the expression (11). The outside radius of the potential is taken as $r_2 = b/\sqrt{\pi}$. As a magnitude of the line charge density within the boundary, the value $\xi = n_s b^2/\Omega$ is accepted.

The calculated values of the residual resistivity due to the grain boundary for different ranges of misorientation are shown in table 3. The low-angle resistivity ρ_g^l/N_g is averaged over the angle interval from 0 to θ^*; the general mean value $\bar{\rho}_g/N_g$ is taken as the average weighted over grain misorientation from 0 to θ_s. For the purpose of comparison the data of the previous calculations [12] and the available experimental results are also represented in table 3.

Table 3. Calculated grain-boundary specific resistivity for different ranges of misorientation.

Metal	ρ_g^l/N_g (10^{-12} Ω cm^2)	ρ_g^h/N_g (10^{-12} Ω cm^2)	ρ_g/N_g (10^{-12} Ω cm^2) This work	Previous work [12]	Experimental data
Na	1.4	6.4	5.0		
K	2.2	10.9	8.4		
Cu	0.5	2.5	2.1	2.2	1.8–3.1 [12]
Ag	0.7	3.3	2.7		
Au	0.7	3.2	2.6	2.8	3.5 [12]
Be	9.4	38.1	27.8		
Zn	5.8	28.3	19.5	27.1	14–55 [34]
Cd	7.0	34.1	23.5	32.6	15.0–19.1 [34]
Al	0.7	3.1	2.6	2.7	2.45 ± 0.1 [39] 1.3–2.5 [34]
Ti	96.7	432.0	309.9		
Zr	97.0	453.3	321.0		
Mo	5.6	28.5	22.0	18.0	12–22 [40]
W	5.6	27.2	21.2	22.0	20 [12]
Fe	4.1	20.4	15.8	6.2	56–~ 260 [41][a]
Co	1.8	8.7	6.0	2.4	5 [12]
Ni	1.5	7.6	6.2	1.9	5.9–14 [12]
Pd	1.9	9.2	7.6		
Pt	2.3	11.0	9.1		

[a] Obtained in [34] by recounting the row of points of figure 2 from [41].

4. Discussion

The results of calculated dislocation residual resistivity presented in table 2 permit one to make a conclusion about the good overall agreement between theory and experiment. The exception is potassium, for which the only estimation of dislocation specific resistivity is known on the basis of the strain dependence of the resistivity. It was made more than 30 years ago and has to be re-examined. Experimental data for Al and Cu are the most reliable. A sufficient number of measurements of electrical resistivity caused by dislocations for these metals have been carried out at different temperatures and by various methods of evaluation of dislocation density. They have been done on both polycrystalline and monocrystalline specimens with diverse degree of deformation. Reasons for the discrepancy in the results have been discussed. It has been established that the measurements performed at 4.2 K and with high density of dislocations ($N_d \sim 10^9$ to 10^{11} cm^{-2}) are most trustworthy. In that case electron–dislocation scattering is predominant and scattering of electrons by phonons and impurities may be neglected. Such a situation arises if $N_d > 10^9$ cm^{-2} at $T = 4.2$ K and if $N_d > 10^{11}$ cm^{-2} at $T = 80$ K [42]. When the dislocation density is not high enough, the measurements result in overestimated values of ρ_d/N_d, possibly by several times. It is apparent from table 2 that our results agree well with available experimental data, especially for those metals whose experimental values one may believe to be most reliable (Cu, Ag, Au, Al, Mo, W). The experimental estimates of dislocation residual resistivity for K, Ti, Zr, Fe, Ni and Pt ought to be considered to be less reliable in our opinion, because they are unique as a rule and were carried out on specimens with comparatively low dislocation density. There are far fewer experimental results for grain boundaries than for dislocations. This is connected with the great complication of such measurements, because in bulk samples the effect is too small, and in film samples it is masked by size and surface effects. However, as follows from table 3, there is quite satisfactory agreement between the calculated quantities ρ_g/N_g and experimental data available in the literature. There is less satisfactory agreement for iron. Partly, this may be accounted for by the fact that iron is a most intricate metal with respect to electron-transfer properties, and it has complicated phase composition that is very sensitive to impurity availability. The phase transformation there happens in the same temperature interval as the processes of recrystallization connected with grain-boundary annealing. There is only a single measurement [41] of the contribution to electrical resistivity caused by grain boundaries in Fe, where a great scatter of quantities ρ_g/N_g has been obtained.

Nevertheless, we may conclude that the proposed dislocation model taking account of the effective number of carriers is the first that allows one to account for the order of dislocation residual resistivity values in transition metals such as Ti, Zr, Mo, W, Fe and Pt and to obtain quite good accordance with experiment for monovalent and polyvalent non-transition metals. Results for grain boundaries presented here agree with experimental data as well as in [12], but the grain-boundary model presented here has dislocation building only in the low-angle range and converts into cylindrical voids with increase of the misorientation angle. It is more realistic in our opinion.

5. Summary and conclusions

The results of the calculation of residual resistivity due to dislocations and grain boundaries, represented in tables 2 and 3, show a quite satisfactory accordance with the available experimental data. Thus, the model of defects proposed here taking into account the lattice

dilatation in the dislocation core, the effective number of carriers and also the existence of resonance electron states near the Fermi energy allowed us to explain the experimental results for a broad range of metals including the transition ones.

Further progress in this direction may be achieved by defining more precisely the effective carrier concentration and the resonance state parameters of the lattice and grain-boundary dislocations on the one hand, and, on the other hand, by means of performing reliably precise measurements of the contribution of these defects to the electrical resistivity of different metals.

Acknowledgments

We are grateful to Professor I D Feranchuck for valuable discussions on the subject of dislocation resonance states. We should also like to thank V M Golub for his help with the numerical calculations.

References

[1] Hanter S C and Nabarro F R N 1953 *Proc. R. Soc.* A **220** 542–61
[2] Stehle H and Seeger A 1956 *Z. Phys.* **146** 217–68
[3] Guyot P 1959 *Acta Metall.* **7** 495–503
[4] Van der Voort E and Guyot P 1971 *Phys. Status Solidi* b **47** 465–73
[5] Seeger A and Bross H 1960 *Z. Naturf.* a **15** 663–89
[6] Harrison W A 1958 *J. Phys. Chem. Solids* **5** 44–6
[7] Brown R A 1977 *J. Phys. F: Met. Phys.* **7** 1283–95
[8] Fockel H-J 1978 *Wiss.-Z. PH Dresden* **12** 49–55
[9] Luhvich A A and Karolik A S 1982 *Fis. Met. Metalloved.* **54** 909–14 (in Russian)
[10] Brown R A 1967 *Phys. Rev.* **156** 889–902
[11] Gantmakher V F and Kulesko G I 1975 *J. Phys.: Condens. Matter* **19** 151–60
[12] Brown R A 1977 *J. Phys. F: Met. Phys.* **7** 1477–88
[13] Molotskiy M I and Rostovtsev V S 1982 *Fiz. Tverd. Tela* **24** 2564–8 (in Russian)
[14] Watts B R 1988 *J. Phys. F: Met. Phys.* **18** 1197–209
[15] Hasson G C, Guillot J B, Baroux B and Goux C 1970 *Phys. Status Solidi* a **2** 551–8
[16] Karolik A S 1988 *Fiz. Met. Metalloved.* **65** 463–70 (in Russian)
[17] Seeger A and Haasen P 1958 *Phil. Mag.* **3** 470–5
[18] Shmatov V T 1975 *Fiz. Met. Metalloved.* **40** 910–19 (in Russian)
[19] Fockel H-J 1987 *Phys. Status Solidi* b **139** 59–66
[20] Brown R A 1982 *Can. J. Phys.* **60** 766–78
[21] Seeger A 1956 *Z. Phys.* **144** 637–48
[22] Nemnonov S A 1965 *Fiz. Met. Metalloved.* **19** 550–68 (in Russian)
[23] Gleiter H and Chalmers B 1972 *High-Angle Grain Boundaries* (Oxford: Pergamon) pp 65–73
[24] Loberg B and Norden H 1976 *Grain Boundary Structure and Properties* ed G A Chadwick and A A Smith (London: Academic) pp 6–14
[25] Smoluchowski R 1952 *Phys. Rev.* **87** 482–7
[26] Vladimirov V I and Orlov A N 1971 *Problem. Prochnosti* **2** 36–8 (in Russian)
[27] Luhvich A A and Karolik A S 1986 *Fiz. Met. Metalloved.* **61** 395–8 (in Russian)
[28] Gleiter H 1977 *Scr. Metall.* **11** 305–9
[29] Sacks R A and Robinson J E 1976 *Phys. Rev.* B **13** 611–20
[30] Blewitt T H, Coltman R R and Redman J K 1955 *Defects in Crystalline Solids* (London: Physical Society) p 309
[31] Basinski Z S, Dugdale J S and Howie A 1963 *Phil. Mag.* **8** 1989–97
[32] Gierrak Z, Moron J W and Lehr A 1983 *Phys. Status Solidi* a **77** 775–83
[33] Shultz H 1959 *Z. Naturf.* a **14** 361–73
[34] Aleksandrov B N, Kan Ya S and Tatishvily D G 1974 *Fiz. Met. Metalloved.* **37** 1150–8 (Engl. Transl. *Phys. Met. Metallogr.* **37** 22–30)

[35] Kopetskii V, Kulesko G I *et al* 1974 *Phys. Status Solidi* a **22** 185–94
[36] Fonteyn D and Pitsi G 1987 *Solid State Commun.* **64** 1113–6
[37] Kovacs I and Nagy E 1965 *Phys. Status Solidi* **8** 795–803
[38] Rider J G and Foxon C T B 1966 *Phil. Mag.* **13** 289–303
[39] Andrews P V, West M B and Robenson C R 1969 *Phil. Mag.* **19** 887–98
[40] Nagano J 1980 *Thin Solid Films* **67** 1–8
[41] Arajs S, Oliver B T and Michalak J T 1967 *J. Appl. Phys.* **38** 1676–7
[42] Koveh M and Wiser N 1983 *J. Phys. F: Met. Phys.* **13** 953–61